

## **Temperature effect on dipolar and exchange interactions for SmCo<sub>5</sub>+1Fe65Co35 nanocomposite powders**

L. P. Muñoz Ortega, J.T. Elizalde Galindo, J.R. Farias Mancilla, C.R. Santillan, and J.A. Matutes Aquino

### **Abstract**

DC magnetization measurements were used to determine the temperature dependencies of the magnetic properties for (90%wt)SmCo<sub>5</sub>+(10%wt)Fe<sub>65</sub>Co<sub>35</sub> nanocomposite powders synthesized by mechanical milling and subsequent annealing. The annealing conditions were T equal to 1073K and time, t, equal to 1.5, 3.0, 4.5, 6.0 min. Maximum magnetization decreased upon cooling in temperature range from 290 to 10 K. Coercivity increased its value to a maximum at the lowest temperature. On the other hand, hysteresis loops collected at low temperatures showed a “knee” in the second quadrant of the demagnetization curve, which suggests that dipolar interactions are becoming stronger than intergrain exchange coupling as temperature is lowered. This low temperature reduction of exchange interactions is confirmed by the temperature dependence of the exchange coupled volume ratio, R. Finally, the temperature effect on magnetic properties is explained on the basis of anisotropy enhancement and reduction of thermal fluctuations as temperature decreases.

### **Introduction**

Since their discovery materials consisting of a mixture of a hard and a soft magnetic nanophase have attracted much attention due to their potential for enhanced maximum energy product (BH)<sub>max</sub> permanent magnet development, and the physical phenomenon in which their unique magnetic properties are based, i.e., exchange

<https://cimav.repositorioinstitucional.mx/jspui/>

coupling.<sup>1-6</sup> Recently, a number of studies have investigated the effect of temperature on exchange coupling and macroscopic properties of composite nanomagnets, but two different explanations for low temperature behavior of exchange coupling has been presented: On one side, the low temperature  $\sigma_r/\sigma_s$  reduction and second quadrant demagnetizing curve “knee” increment observed has been attributed to exchange “decoupling” due to diminishing of exchange length at lower temperatures.<sup>7,8</sup> On the other side, because of the high remanence and coercivity values, the second quadrant demagnetizing curve distortion is attributed only to a pronounced difference between the temperature dependencies of the anisotropy constants of the hard and soft phases.<sup>9</sup> In this work, we present our findings in the low temperature effect in magnetic properties and interactions of nanocomposite  $\text{SmCo}_5+\text{Fe}_{65}\text{Co}_{35}$ , where the temperature dependence of the exchange coupled volume ratio,  $R$ , is presented to explain a low temperature decoupling.

### **Experimental methodology**

Raw material ingots of Sm, Co, and Fe with purity of 99.9%, 99.9%, and 99.8%, respectively, were used to produce small buttons of  $\text{SmCo}_5$  and  $\text{Fe}_{65}\text{Co}_{35}$  by arc melting under Ar atmosphere. The buttons were turned and re-melted four times to ensure homogeneity, and then coarsely pulverized and mixed to obtain about 3 g of  $\text{SmCo}_5$  (90%wt)+ $\text{Fe}_{65}\text{Co}_{35}$  (10%wt) powders. After, the powders were mechanically milled for 240 min under Ar atmosphere using a SPEX 8000 ball mill with a ball-to-powder ratio of 8:1. The as-milled amorphous material was annealed at 1073K for 1.5, 3.0, 4.5, and 6.0 min in high vacuum Vycor tubes, followed by quenching in water. X-ray diffraction (XRD) patterns were obtained using a Panalytical X'Pert MPD diffractometer

<https://cimav.repositorioinstitucional.mx/jspui/>

with Cu-K $\alpha$  radiation in a  $2\theta$  ranging from  $20^\circ$  to  $65^\circ$ , with a step size of 0.016 and time per step of 30 s. Transmission electron microscopy (TEM) pictures, and energy dispersive spectroscopy (EDS) for elemental composition were obtained in a Jeol JEM-2200FS. Magnetic hysteresis loops were measured on a Quantum Design Physical Property Measurement System in fields up to 40 kOe at temperature, T, ranging from 290 to 10 K.

## Results and discussion

Figure 1 shows XRD patterns obtained at room temperature for samples (a) as-milled, and annealed at 1073K for (b) 1.5, (c) 3.0, (d) 4.5, and (e) 6.0 min. All phases in samples were identified with SmCo<sub>5</sub> (PDF2-00-027-1122), Fe<sub>65</sub>Co<sub>35</sub> (PDF2-00-048-1817), SmO (PDF2-00-006-0440), and Fe (PDF2-00-034-0529). The as-milled samples exposed an amorphous-like XRD pattern. Iron was present at lower annealing times, samples (b) and (c). SmO increases its presence for the longest annealing time. Average crystallite size values calculated with Scherrer's formula<sup>10</sup> for SmCo<sub>5</sub> and Fe<sub>65</sub>Co<sub>35</sub> from 3.0 min annealed sample's XRD pattern were 13 and 56 nm, respectively.

In order to explore the effect of temperature on magnetic properties, and because of XRD patterns and room temperature hysteresis loops, not shown here, the 3.0 min annealed sample was selected to carry out TEM analysis and DC magnetometry. Figure 2 shows high resolution TEM image for the edge of a nanoparticle, where SmCo<sub>5</sub> and Fe<sub>65</sub>Co<sub>35</sub> were identified from EDS spectrum and interlayer spacing values. The observed fringes correspond to plane (100) and (101) for SmCo<sub>5</sub> and Fe<sub>65</sub>Co<sub>35</sub>, respectively. The image exposed that grains of both phases, hard and soft, are adjacent

<https://cimav.repositorioinstitucional.mx/jspui/>

in the well defined microstructure. At the edge of the nanoparticles, average crystallite sizes were 7 and 4 nm for  $\text{SmCo}_5$  and  $\text{Fe}_{65}\text{Co}_{35}$ , respectively.

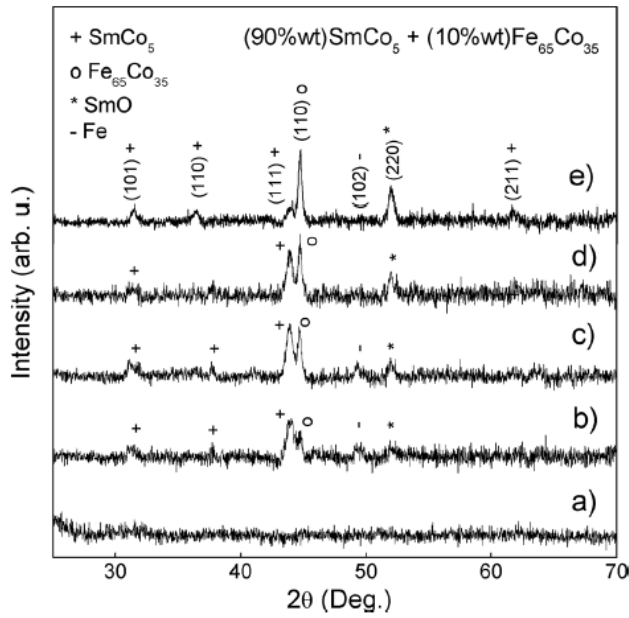


FIG. 1. XRD patterns obtained at room temperature for (a) as-milled, and annealed at 1073 K for (b) 1.5, (c) 3.0, (d) 4.5, and (e) 6.0 min samples.

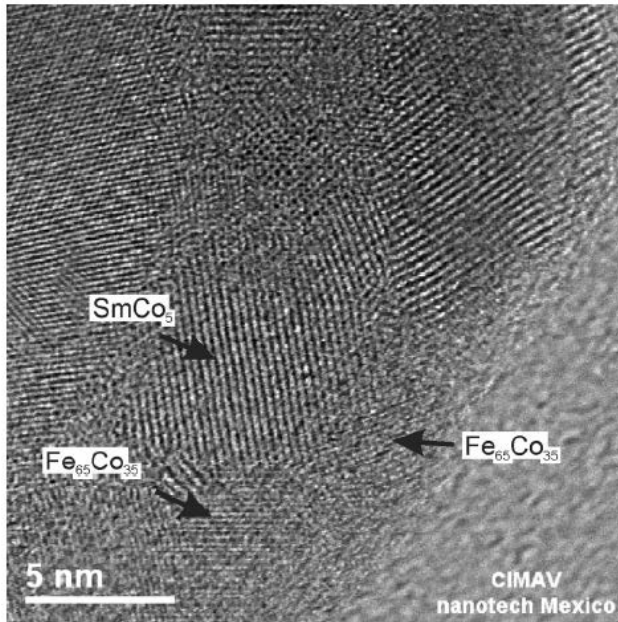


FIG. 2. High resolution TEM image for the edge of a nanoparticle of  $(90\text{wt})\text{SmCo}_5 + (10\text{wt})\text{Fe}_{65}\text{Co}_{35}$ .

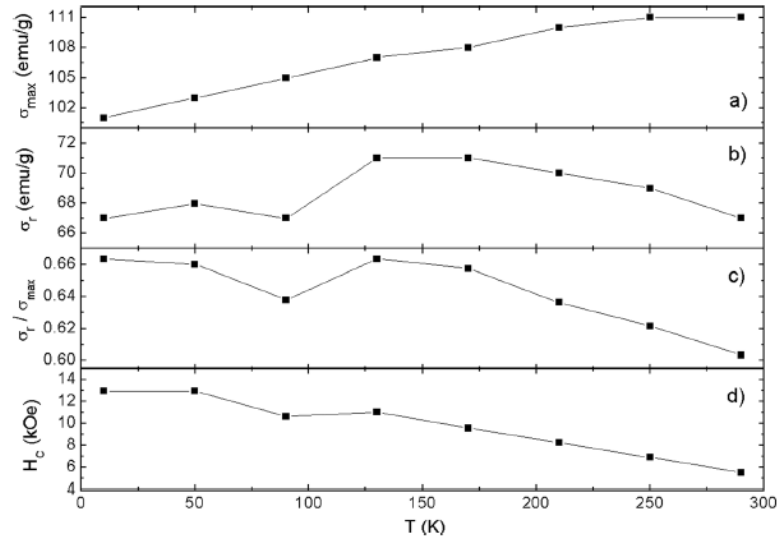


FIG. 3. Magnetic properties behavior of (90%wt)  $\text{SmCo}_5$  + (10%wt)  $\text{Fe}_{65}\text{Co}_{35}$  nanopowders annealed at 1073 K for 3.0 min in temperature range between 290 and 10 K (a)  $\sigma_{max}$ ; (b)  $\sigma_r$ ; (c)  $\sigma_r/\sigma_{max}$ ; and (d)  $H_c$ .

Figure 3 shows maximum magnetization,  $\sigma_{max}$ , remanence,  $\sigma_r$ , remanence to maximum magnetization ratio,  $\sigma_r/\sigma_{max}$ , and coercivity,  $H_c$ , behavior of (90%wt)  $\text{SmCo}_5$  +(10%wt)  $\text{Fe}_{65}\text{Co}_{35}$  nanopowders annealed at 1073K for 3.0 min in temperature range between 290 and 10K. The data show that  $\sigma_{max}$  decrease close to 10% upon cooling. Meanwhile, due to thermal energy reduction when cooling,  $\sigma_r$  increase up to a maximum at 130 K, and then, starts decreasing to its room temperature value as temperature reaches 10 K. On the other hand,  $H_c$  increases by more than 100% when temperature is lowered from 290 to 10 K. This behavior can be attributed to the temperature dependence of magnetocrystalline anisotropy of  $\text{SmCo}_5$  hard phase,<sup>11</sup> which is the underlying responsibility for coercivity.

Figure 4 shows the hysteresis loops of (90%wt)  $\text{SmCo}_5$  +(10%wt)  $\text{Fe}_{65}\text{Co}_{35}$  nanopowders annealed at 1073K for 3.0 min in temperature range between 290 and 10 K. The demagnetizing curve at 290K has a smooth convex profile that, according to Kneller and Hawig,<sup>12</sup> correspond to a fully exchange coupled nanocomposite. Meanwhile, as temperature decreases, the hysteresis loop profile exhibits a “knee” in

<https://cimav.repositorioinstitucional.mx/jspui/>

the second quadrant. As mentioned before, this feature has been interpreted as an exchange decoupling,<sup>7,8</sup> while others have indicated that such “decoupling” cannot occur together with an enhancement of magnetic properties, like coercivity, upon cooling.<sup>9</sup> To clarify this behavior, exchange coupled volume ratio  $R$  can be used, as introduced by Dahlgren and Grössinger,<sup>13</sup>

$$R = \frac{V_{\text{coupled}}}{V_{\text{total}}} = 1 - \left(1 - 2\frac{l_{\text{ex}}}{D}\right)^3, \quad (1)$$

where  $l_{\text{ex}}$  and  $D$  are effective exchange length and average crystal size (for two phases), respectively.<sup>1,13</sup> As indicated for Eq. (1),  $R$  means the volume ratio that is exchange coupled for a given average crystallite size. Since the latter is constant upon temperature, the only physical responsibility for any change in  $R$ , as temperature decreases, is the effective exchange length, i.e., the magnetocrystalline anisotropy constant. Therefore, in samples with temperature dependent magnetocrystalline anisotropy constant, it can be expected exchange decoupling under cooling. As shown at the insert of Fig. 4,  $R$  reduces as temperature decreases, in good agreement with the “knee” enhancement observed, exposing an exchange coupling decrement, with a corresponding increment of dipolar interactions.

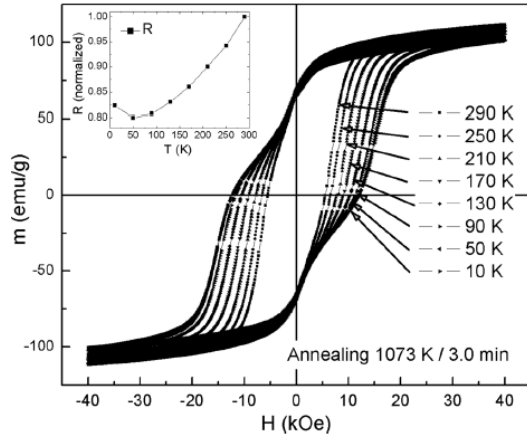


FIG. 4. Hysteresis loops of (90%wt)  $\text{SmCo}_5$  + (10%wt)  $\text{Fe}_{65}\text{Co}_{35}$  nanopowders annealed at 1073 K for 3.0 min in temperature range between 290 and 10 K. Insert shows R behavior upon cooling.

## Conclusions

In summary, DC magnetization measurements carried out in selected samples exposed a very interestingly behavior under cooling. The characteristic “knee” enhancement observed in the second quadrant demagnetizing curve upon cooling expose an exchange decoupling between adjacent nanocrystals. Finally, the underlying physical responsibility for this behavior, exposed by using the exchange coupled volume ratio  $R$ , was found to be the magnetocrystalline anisotropy constant dependence on temperature.

## Acknowledgments

The authors want to thank to UACJ for the support to carry out this research and Carlos Ornelas from Laboratorio Nacional de Nanotecnología from CIMAV for the studies of HRTEM.

## References

- 1.- R. Skomski and J. M. D Coey, Phys. Rev. B 48, 15812 (1993).
- 2.- I. A. Al-Omari and D. J. Sellmyer, Phys. Rev. B 52, 3441 (1995).

<https://cimav.repositorioinstitucional.mx/jspui/>

- 3.- A. Manaf, R. A. Buckley, and H. A. Davies, *J. Magn. Mater.* 128, 302 (1993).
- 4.- R. Fischer, T. Schrefl, H. Kronmüller, and J. Fidler, *J. Magn. Mater.* 153, 35 (1996).
- 5.- G. McCormick, W. F. Miao, P. A. I. Smith, J. Ding, and R. Street, *J. Appl. Phys.* 83, 6256 (1998).
- 6.- K. J. Strnat, *Proc. IEEE* 78, 6 (1990).
- 7.- J. P. Liu, R. Skomski, Y. Liu, and D. J. Sellmyer, *J. Appl. Phys.* 87, 6740 (2000).
- 8.- J. T. Elizalde Galindo, A. W. Bhuiya, F. Rivera Gomez, J. A. Matutes Aquino, and C. E. Botez, *J. Appl. Phys.* 41, 095008 (2008).
- 9.- J. H. Yin, Z. G. Sun, Z. R. Zhang, H. W. Zhang, and B. G. Shen, *J. Appl. Phys.* 89, 8351 (2001).
- 10.- O.B. D. Cullity and S. R. Stock, *Elements of X-Ray Diffraction*, 3rd ed. (Prentice-Hall, New York, 2001).
- 11.- S. G. Sankar, V. U. S. Rao, E. Segal, W. E. Wallace, W. G. D. Frederick, and H. J. Garrett, *Phys. Rev. B* 11, 435(1975).
- 12.- E. F. Kneller and R. Hawig, *IEEE Trans. Magn.* 27, 3588 (1991).
- 13.- M. Dahlgren and R. Grossinger, *Mater. Sci. Forum* 302–303, 263 (1999).